

04,06,13

Single crystals $(\text{Na}_{1/2}\text{Bi}_{1/2})(\text{Mg}_{1/3}\text{Nb}_{2/3})\text{O}_3$: synthesis, structure, properties

© P.P. Syrnikov, V.G. Zalesskiy, N.V. Zaitseva, A.V. Khalipov, A.I. Fedoseev, S.G. Lushnikov

Ioffe Institute,
St. Petersburg, Russia
E-mail: nsh@mail.ioffe.ru

Received September 7, 2024

Revised September 8, 2024

Accepted September 9, 2024

Single crystals $(\text{Na}_{1/2}\text{Bi}_{1/2})(\text{Mg}_{1/3}\text{Nb}_{2/3})\text{O}_3$ (NBMN) of perovskite with disordering in A and B sublattices were grown for the first time by spontaneous crystallization. The space group of the NBMN crystal ($Pm\bar{3}m$, $a = 3.954 \pm 0.001 \text{ \AA}$) and the value of the refractive index ($n = 2.31 \pm 0.02$, $\lambda = 0.633 \mu\text{m}$) at room temperature were determined. Anomalies were found in the temperature dependences of the dielectric response in NBMN: frequency-dependent maxima of dielectric losses in the temperature range 110 K, characteristic of the transition to a relaxor ferroelectric state and a frequency-independent anomaly in the vicinity of 300 K. The existence of thermally activated conduction behavior with an activation energy of 0.66 eV at temperatures above 590 K is shown. The measurement of dielectric hysteresis by the PUND method revealed the existence of switchable polarization at 77 K. The analysis of the dielectric properties makes it possible to attribute the NBMN crystal to the family of relaxor ferroelectrics with a perovskite structure.

Keywords: Ferroelectrics, crystal lattice dynamics, polarization, dielectric properties.

DOI: 10.61011/PSS.2024.10.59626.232

1. Introduction

Partially disordered perovskites with the general formula of $A'A''B''\text{O}_3$ are actively studied as a result of the broad practical application of many compounds from this family, so is the fundamental interest of researchers in the effect of disordering on the dynamics of the crystal lattice. Relaxor ferroelectrics (relaxors) belong to this family of perovskites and are characterized by a wide frequency-dependent permittivity anomaly stretched by hundreds of degrees, generally unrelated to the structural phase transition [1,2]. The mechanisms of occurrence of the anomaly of the dielectric response and the relaxor ferroelectric state have been discussed for more than 60 years since the synthesis of the first compounds [3]. More than 1000 compounds from this family are known to date. They were synthesized on the basis of such classical representatives of relaxors as $\text{PbMg}_{1/3}\text{Nb}_{2/3}\text{O}_3$ (PMN), $\text{PbZn}_{1/3}\text{Nb}_{2/3}\text{O}_3$ (PZN), $\text{PbSc}_{1/2}\text{Nb}_{1/2}\text{O}_3$ (PSN), $(\text{Na}_{1/2}\text{Bi}_{1/2})\text{TiO}_3$ (NBT) and others [1–5], however, it has not been possible so far to grow stoichiometric crystals (not based on solid solutions) in which the disordering of two perovskite sublattices is realized simultaneously (A and B). The gigantic values of the piezoelectric response and the unique dielectric properties of relaxors have long been used in capacitor engineering, optoelectronics, and other areas of high-tech industry. A number of compounds from this family have been recently considered as materials for electrocaloric cooling elements [6], energy storage devices integrated into chips [7] and others [8,9]. A limiting factor for the development of technologies for creating various devices

using these materials is that most of the relaxors are lead-containing compounds, the use of which is recognized as environmentally harmful. Therefore, the problem of synthesis of new lead-free relaxor compounds is extremely relevant. This paper presents the results of synthesis and study of the physical properties of a single crystal of a new perovskite $(\text{Na}_{1/2}\text{Bi}_{1/2})(\text{Mg}_{1/3}\text{Nb}_{2/3})\text{O}_3$ (NBMN), which does not contain lead ions and has a partial disordering in both the A- and B-sublattice. NBT and PMN crystals were „progenitors“ of this new compound which were used as models for studying the relaxation state in perovskites with disordering in A or B sublattices, respectively.

NBT crystals contain two ions Na^{2+} and Bi^{2+} in the A-sublattice of perovskite [1] and are one of the few representatives of relaxors with this type of disordering. The first studies of the physical properties of NBT were conducted in the late 50s. The dynamics of the lattice of NBT crystals demonstrates a nontrivial sequence of structural phase transitions and transformations in which ferroelastic, ferroelectric and relaxor states arise [10–13]. The crystal structure of NBT is characterized by cubic symmetry at temperatures above $\sim 813 \text{ K}$ (space group $Pm\bar{3}m$). An antiferrodisorsion phase transition of the first order takes place in case of cooling, while the symmetry of the crystal decreases from cubic to tetragonal $P4bm$ [14]. An anomaly of dielectric susceptibility ϵ' is observed in the form of a wide maximum in case of further cooling below 800 K in NBT at low test frequencies. The maximum value of ϵ' reaches 10^3 – 10^4 , and its magnitude and temperature strongly depend on frequency [15]. The structural changes of the NBT crystal are quite complex below 740 K and are the subject of wide discussion: For instance, high-resolution

electron microscopy [14] has shown the possibility of the existence of an intermediate orthorhombic phase separating the tetragonal and rhombohedral ferroelectric phases in addition to the assumption of the coexistence of tetragonal and rhombohedral phases [16]. The second anomaly of the dielectric constant is observed in the form of a wide maximum in the vicinity of the temperature of ~ 620 K. The dielectric susceptibility ceases to depend on frequency at $T < 620$ K. Rhombohedral symmetry was first assumed ($R3c$) for temperatures below ~ 523 K in NBT crystals, and later monoclinic symmetry (C_c) or their coexistence was also proposed based on X-ray diffraction experiments [16]. The dielectric constant is again accompanied by a relatively small frequency dispersion in the same temperature range [15,17]. NBT becomes a ferroelectric below 470 K, for which estimations of the coercive field and residual polarization give the following values: $E_c = 73$ kV/cm and $P_r = 38 \mu\text{C}/\text{cm}^2$ [18–20]. The study of the dielectric properties of NBT was published in numerous papers which have some discrepancy in experimental data of phase transition temperatures and temperature dependences of dielectric parameters [15]. This may be attributable to the technology of crystal growth: growth from a melt or the Czochralski method [21]. The polarization of NBT crystals is hampered by a large coercive field and high conductivity (compared to lead-containing piezoelectrics), which is the main obstacle for a broad practical application [21–23]. Currently the effect of additional impurity ions that replace Bi and Na ions in the A position, or Ti ions in the B position is studied, or the synthesis of ceramics of complex solid solutions based on NBT is conducted for improvement of NBT piezoelectric properties [22–25].

PMN relaxor ferroelectric represents another type of perovskite disordering, in which there is an unordered distribution of two dissimilar cations Mg^{2+} and Nb^{5+} in the B-sublattice of the crystal [1,3]. A diffuse phase transition is observed in PMN, which is accompanied by an anomaly of dielectric properties in the form of a wide and frequency-dependent maximum of dielectric susceptibility with a value of $\epsilon'(10 \text{ kHz}) = 2 \cdot 10^4$ at $T_{\text{max}} = 275$ K [1,4]. At the same time, the PMN structure remains cubic up to helium temperatures.

The first reports on the attempt to synthesize compounds with disordering in both A- and B-sublattices based on PMN and NBT were published in Ref. [23,25], which provide data on the synthesis and properties of piezoelectric ceramics of $\text{Bi}_{1/2}\text{Na}_{1/2}(\text{Mg}_{1/3}\text{Nb}_{2/3})\text{O}_3$ (BNMN) and $\text{Bi}_{1/2}\text{Na}_{1/2}(\text{Ti}_{(100-x)}(\text{Mg}_{1/3}\text{Nb}_{2/3})_x)\text{O}_3$, respectively. The dielectric constant was 250 at room temperature at a frequency of 1 kHz and showed a slight increase, no more than 20%, when heated from 300 to 730 K, without any significant anomalies. The polarization of ceramics was limited by a breakdown field of 45 kV/cm. Ferroelectric hysteresis loops (P–E loops) obtained using the traditional Sawyer–Tower method had a strongly distorted shape and residual polarization was not found. The value of the piezomodule d_{33} after preliminary polarization of BNMN

ceramics in the pre-breakdown field was estimated at 1.8 pC/N [25]. We have not found any other information about the attempt to synthesize compounds with the general formula $A'A''B'B''\text{O}_3$ in the literature.

The aim of this paper is to grow single crystals of perovskite $(\text{Na}_{1/2}\text{Bi}_{1/2})(\text{Mg}_{1/3}\text{Nb}_{2/3})\text{O}_3$ –(NBMN) and study its structure and dielectric properties over a wide temperature range.

2. Synthesis and research methods

Crystals were synthesized and grown by the method of spontaneous crystallization. The initial components NaBiO_3 , MgO , Nb_2O_5 and B_2O_3 were placed in a platinum crucible, heated to 1250°C , held for 3 hours at this temperature and subsequently cooled for two weeks. Transparent light yellow crystals of cubic shape with 5–8 mm side dimensions were obtained in the result. The elemental composition of NBMN crystals was confirmed by X-ray spectral microanalysis using „CAMEBAX“ microanalyzer.

A sample which had a developed (001) surface with an area of 6 mm^2 polished to optical quality and coated with silver electrodes was prepared for dielectric measurements. The thickness of the dielectric layer of the capacitor structure was 1 mm. The temperature dependence of the complex dielectric constant was measured using GoodWill LCR-819 impedance meter in a field with an amplitude of 1 V, in the frequency range of 0.1–100 kHz and in the temperature range from 77 to 800 K. The DC-conductivity was measured using teraohmmeter E6-13A.

The dielectric hysteresis loops were measured using the Merz circuit. The current passing through the sample was measured using a nanovoltmeter based on the voltage drop with the measuring resistance of 100 k Ω . A high-voltage source SRS-350 controlled by a computer was used to create high-voltage triangular pulses with an amplitude up to 2 kV and a duration of 30 s.

3. Experimental results and discussion

3.1. NBMN crystal structure

NBMN crystals were optically isotropic at room temperature and the refractive index determined by the Brewster angle was estimated at $n = 2.31 \pm 0.02$ at a wavelength of $\lambda = 0.633 \mu\text{m}$. Powder diffraction obtained using X-ray diffractometer „Dron-3“ determined the symmetry of the crystal structure as cubic, space group $Pm\bar{3}m$, with lattice constant $a = 3.954 \pm 0.001 \text{ \AA}$ (Figure 1).

3.2. Dielectric permittivity

Figure 2 shows the temperature dependences of the real and imaginary parts of the complex dielectric constant $\epsilon^* = \epsilon' - i\epsilon''$ for different frequencies in the NBMN crystal. At room temperature, the dielectric constant of NBMN

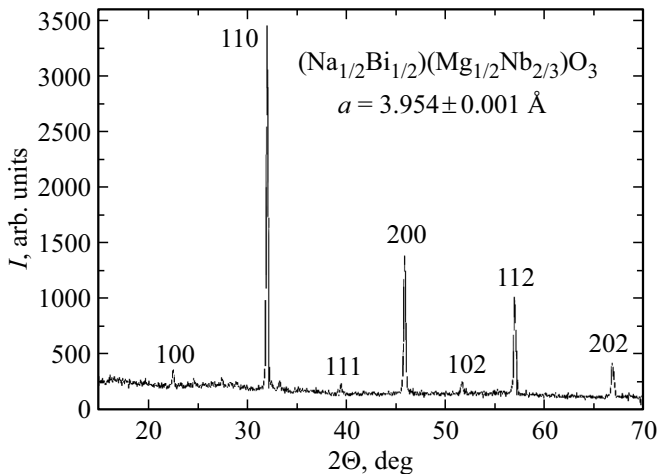


Figure 1. Powder diffraction pattern $(\text{Na}_{1/2}\text{Bi}_{1/2})(\text{Mg}_{1/3}\text{Nb}_{2/3})\text{O}_3$ obtained at room temperature.

at a frequency of 1 kHz is $\varepsilon' = 230$, the loss tangent is $\text{tg } \delta = 0.01$ (for comparison, NBT parameters: $\varepsilon' = 750$, $\text{tg } \delta = 0.05$ [17]). The temperature behavior of $\varepsilon'(\omega, T)$ can be conditionally divided into three regions: high-temperature, at $T > 400$ K, the region from 400 to 200 K and low-temperature ($T < 200$ K). An increase of ε' is observed in the high temperature region, at $T > 420$ K, accompanied by significant frequency dispersion — a significant increase of the values of ε' at low frequencies, and it practically disappears at high frequencies (Figure 2, *a*). This dispersion ε' is not observed in the second section (from 400 to 250 K) of the dependence $\varepsilon'(\omega, T)$, which demonstrates a wide maximum with a noticeable break in the temperature dependence $\varepsilon'(T)$ in the vicinity of 300 K. In the temperature range of 250–90 K, a weak dispersion of the dielectric constant is observed (Figure 2, *a*). It is possible that there are two fairly wide anomalies in the vicinity of 150 and 300 K in the temperature dependence $\varepsilon'(\omega, T)$ in NBMN at $T < 350$ K, the superposition of which is observed by us in the temperature behavior $\varepsilon'(\omega, T)$ at $T < 350$ K. It is possible to note a similar behavior of the dielectric constant in a NBT single crystal observed in a different temperature range: a wide maximum ε' at 620 K with a large frequency dispersion in the high-temperature region, in the absence of dispersion in the temperature range of 520–620 K and the appearance of a small maximum and weak dispersion ε' at temperatures below 520 K [15,17].

The temperature dependence of the imaginary part of the dielectric constant $\varepsilon''(\omega, T)$ in an NBMN crystal is shown in Figure 2, *b*. The presented temperature behavior $\varepsilon''(\omega, T)$ can also be divided into high- and low-temperature regions. A nonlinear increase of the value of ε'' is observed with the increase of the temperature in Figure 2, *b*, in the high-temperature region (at $T > 450$ K). Just as for $\varepsilon'(\omega, T)$, an increase of frequency results in the decrease of the values of $\varepsilon''(\omega, T)$, while a wide maximum becomes noticeable in the vicinity of $T_1 \approx 550$ K at high frequencies.

Two anomalies are clearly visible in the low-temperature region of dependence $\varepsilon''(\omega, T)$: a frequency-independent maximum in the vicinity of 300 K and a wide maximum in the vicinity of $T_m \approx 110$ K at a frequency of 1 kHz, the position of which shifts to the high temperature region with the increase of the frequency (Figure 2, *b*). The anomaly in the vicinity of $T_2 \approx 300$ K in the behavior of $\varepsilon''(\omega, T)$ is masked at high frequencies by the shift of the maximum T_m to the high temperature region, but it is clearly visible at low frequencies.

The dependence of the maximum temperature T_m on the frequency observed in dependence $\varepsilon''(\omega, T)$ was plotted in the insert to Figure 2, *b* and was approximated using the Arrhenius law $\omega = \omega_0 \exp[-E_a/kT_m]$ and Vogel–Fulcher law $\omega = \omega_0 \exp[-E_a/k(T_m - T_F)]$, where: ω_0 — frequency of hopping attempts, E_a — activation energy of charge carriers, k — Boltzmann constant, T_m — maximum temperature and T_F — „freezing“ temperature or Vogel–Fulcher

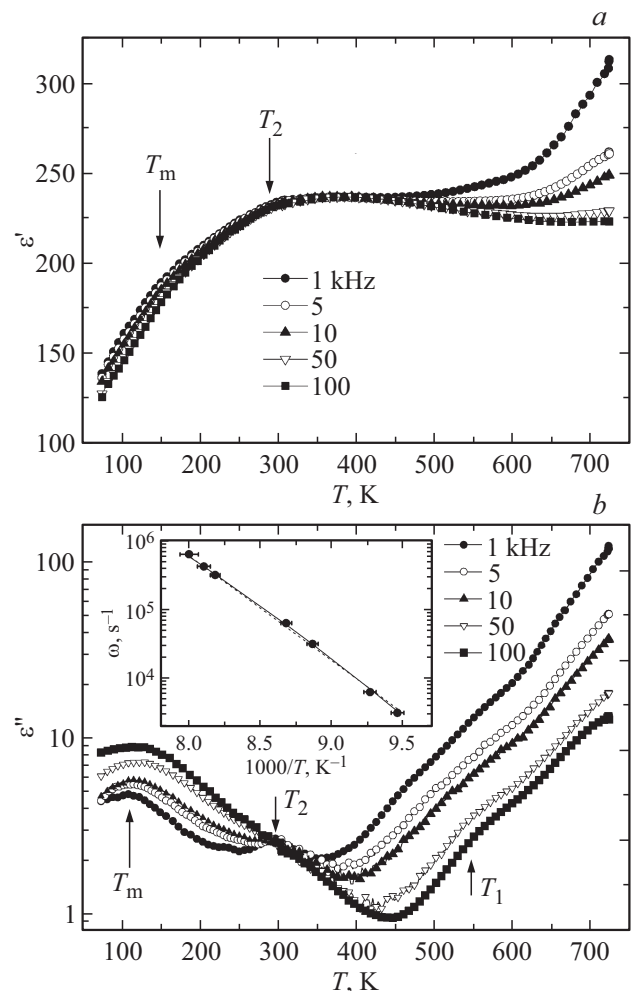


Figure 2. Temperature dependence of the real (*a*) and imaginary (*b*) parts of the dielectric constant of an NBMN crystal at different frequencies. The insert to Figure 2, *b* shows the dependence of the maximum temperature T_m on frequency (the dependence according to the Arrhenius law is shown by the dotted line, the Vogel–Fulcher dependence is shown by the solid line).

temperature. The best results were achieved by approximating the dependence in the insert to Figure 2, *b* using the expression for Vogel–Fulcher law, with the values: $E_a = 1.1$ eV, $\omega_0 = 7 \cdot 10^{12} \text{ s}^{-1}$ and $T_F = 45$ K, while unrealistic values of the corresponding parameters were obtained for the Arrhenius law: $E_a \approx 3$ eV and $\omega_0 \approx 10^{17} \text{ s}^{-1}$. The dependence T_m on the measurement frequency obtained using this description is in good agreement with the classical behavior $T_m(\omega)$ for relaxors [5].

If we compare the nature of the dispersion on the temperature dependence of the imaginary part of the dielectric constant (Figure 2, *b*) separately for high and low temperatures, it can be noted that in the first case the losses are greater at low frequencies, and in the second case the losses are higher at high frequencies. The value $d\varepsilon''/d\omega$, the dispersion of the imaginary dielectric susceptibility, changes the sign in the temperature range of 300–350 K, which indicates a change in the mechanism of dielectric losses. The Maxwell–Wagner relaxation can serve as such a mechanism for high temperatures [26]. Dielectric losses are determined by the polarization characteristics of relaxor ferroelectrics in the case of low temperatures [1]. Apparently, the change of the sign of dispersion $d\varepsilon''/d\omega$ in the temperature range of 290–350 K is associated with a change of the phase state of the crystal.

3.3. Conductivity

The analysis of the temperature dependences of AC and DC-conductivity $\sigma_{ac}(\omega, T)$ and $\sigma_{dc}(T)$ is a fairly convenient way to identify the mechanism of behavior of dielectric losses ε'' at different frequencies and temperatures [26]. It is necessary for this purpose to perform transformations of the imaginary permittivity according to the formula $\sigma_{ac}(\omega, T) = \omega\varepsilon_0\varepsilon''(\omega, T)$. Then the total conductivity $\sigma(\omega, T)$ consists of two values:

$$\sigma(\omega, T) = \sigma_{dc}(T) + \sigma_{ac}(\omega, T),$$

where σ_{dc} — through conductivity at a frequency of $\omega = 0$, determined by the drift of free charges in a constant field (active conductivity) and σ_{ac} — conductivity associated with dielectric losses (reactive conductivity) [26].

Figure 3, *a* shows the temperature dependences for the DC-conductivity and AC-conductivity of the NBMN single crystal at different frequencies. The figure shows the dispersion of conductivity, the value of which increases with increasing frequency. A decrease in the dispersion of AC-conductivity is observed in the temperature range above 590 K. The behavior of $\sigma_{ac}(\omega, T)$ at $T > 650$ K is similar to the temperature dependence of $\sigma_{dc}(T)$. The same behavior of AC-conductivity is observed in NBT single crystals in the temperature range (above 620 K), where the contribution to the dielectric response of Maxwell–Wagner relaxation becomes significant [17]. Two linear sections are clearly visible in the high-temperature behavior of $\sigma_{ac}(\omega, T)$ in Figure 3, *b*. The temperature region at $T > 650$ K is of the greatest

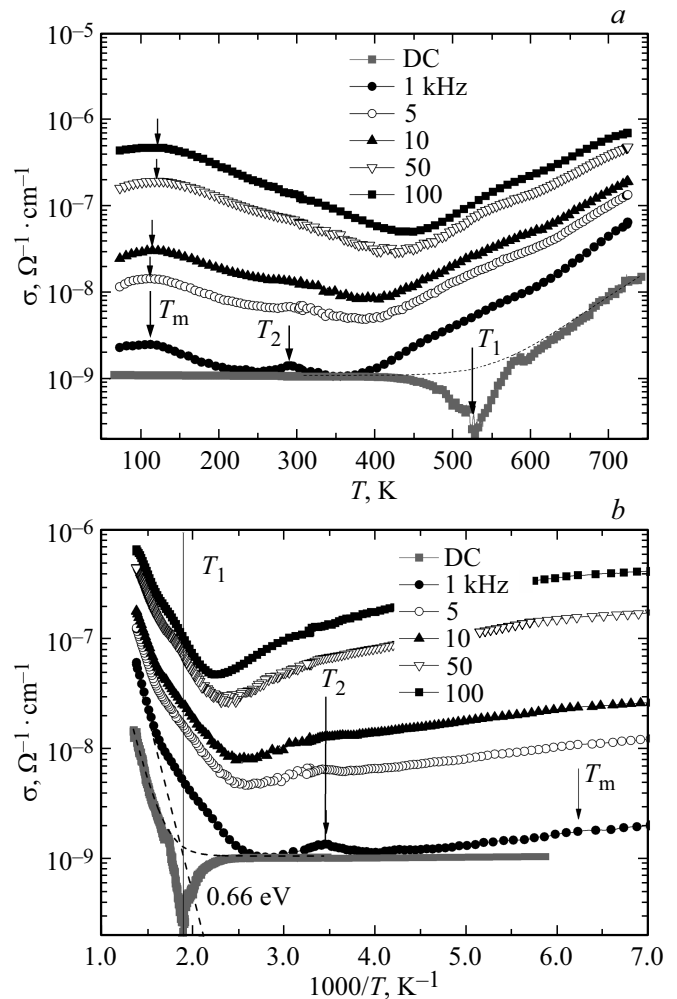


Figure 3. Temperature dependences of AC and DC-conductivity in an NBMN crystal: *a*) — on a semi-logarithmic scale and *b*) — in axes corresponding to the Arrhenius law. Dotted lines match with the thermal activation law, arrows indicate the position of frequency-dependent maxima of AC-conductivity.

interest, the slope angles of the dependencies $\sigma_{ac}(\omega, T)$ and $\sigma_{dc}(T)$ are practically the same and match well with the thermal activation law $\sigma_{dc}(T) = \sigma_0 \exp -E_a/kT$, where: σ_0 — constant, E_a — activation energy of charge carriers, k — Boltzmann constant. The following parameters were obtained for NBMN crystals: $\sigma_0 = 5 \cdot 10^{-4} \Omega^{-1} \cdot \text{cm}^{-1}$ and $E_a = 0.66$ eV. For comparison, the activation energy is estimated at 0.7–0.9 eV in NBT crystals, as a result of the conducted conductivity analysis [17]. The situation with the behavior of conductivity in the temperature range from 430 to 650 K is more complicated. An anomaly in DC-conductivity is clearly visible in Figure 3, *b* in the form of a minimum in the vicinity of 530 K, at which the conductivity decreases by almost an order of magnitude, to $\sigma_{dc} = 10^{-10} \Omega^{-1} \cdot \text{cm}^{-1}$. This anomaly is not observed in temperature dependencies $\sigma_{ac}(\omega, T)$. Instead, we see an almost linear dependence $\sigma_{ac}(\omega, T)$ in the discussed

temperature range (Figure 3, *b*). The reason for this abnormal conduction behavior requires additional study.

Figure 3 shows two anomalies in the low-temperature region depending on $\sigma_{ac}(\omega, T)$: a maximum in the vicinity of $T_2 \approx 300$ K and a wide, frequency-dependent maximum in the vicinity of $T_m \approx 110$ K. The maximum of AC-conductivity at T_2 is clearly visible at low frequencies, masked by an increase of conductivity values and a shift to the high-temperature region of a wide frequency-dependent maximum at T_m at high-frequency temperature dependences.

Another feature of DC-conductivity in NBMN is its relatively high value for dielectrics with a perovskite structure at direct current $\sigma_{dc} = 1 \cdot 10^{-9} \Omega^{-1} \cdot \text{cm}^{-1}$ (at $T = 300$ K, $U = 10$ V), as well as the accumulation of space charge which causes a reversible breakdown. Samples with a thickness of 1 mm withstood a field of 20 kV/cm for 1 min at a temperature of 77 K, the breakdown began in a field of 10 kV/cm at a temperature above 400 K, and the breakdown field decreased to 90 V/cm at a temperature of 700 K.

3.4. Measurement of hysteresis loops

Ferroelectric hysteresis loops were measured at a temperature of 77 K using the PUND (Positive Up, Negative Down) method [27]. Unlike the traditional loop measurement method, the dielectric is polarized in this method by a series of external field pulses consisting of two consecutive pulses of the same polarity (pulses 1–2 in Figure 4), then by two identical pulses of a different polarity (pulses 3–4).

The application of this method makes it possible to distinguish the current associated with polarization switching from the total current, which consists of the conduction current J_b and the displacement current J_s . In turn, the displacement current consists of the current of reversible polarization of the dielectric and the switching current of spontaneous polarization. All the listed current components,

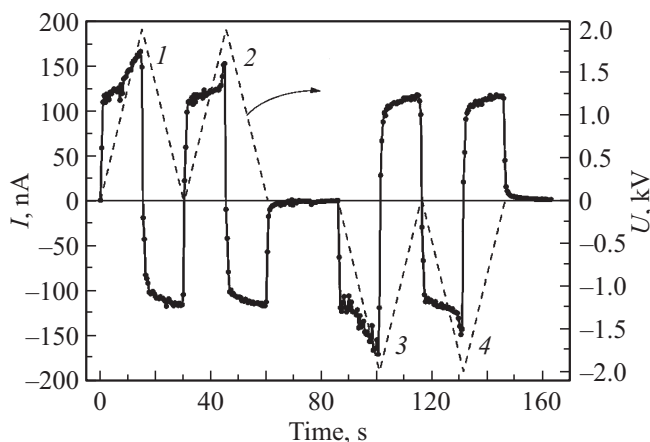


Figure 4. Measurement of the polarization of the NBMN sample by PUND method. Current pulses are shown as a response to a series of triangular-shaped high voltage pulses (shown with a dashed line).

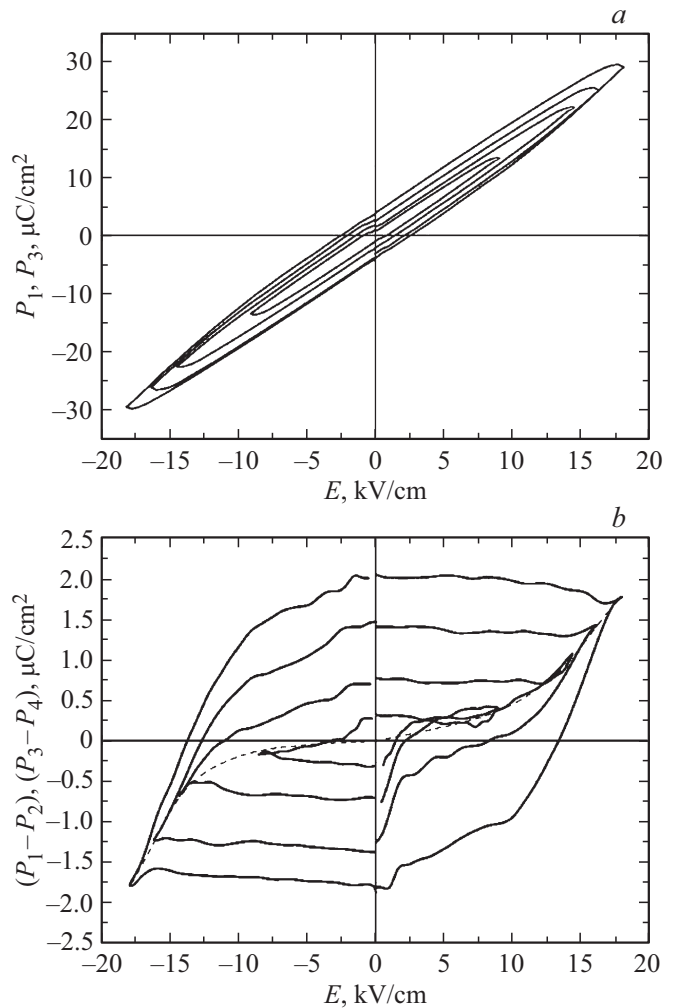


Figure 5. P–E hysteresis loops in an NBMN crystal: *a*) a general polar response, including all contributions from polarization and conductivity, *b*) a polar response associated only with polarization switching. The dotted line shows the dependence of the maximum polarization on the field.

including contributions related to polarization switching, are contained in the first positive and first negative current density pulses J_1 and J_3 , after integration of which P–E hysteresis loops can be obtained. The shape of the hysteresis loop in the NBMN crystal, shown in Figure 5, *a*, is characteristic of a dielectric with a significant contribution of conductivity. The second positive and second negative current density pulses (J_2 and J_4) also include the contribution of the conduction current, but these pulses do not include polarization switching current. Therefore, it is sufficient to use the differences in the values of current pulses J_1 – J_3 and J_2 – J_4 for obtaining loops containing switchable polarization data.

Figure 5, *b* shows hysteresis loops of switchable polarization in BMNM at a temperature of 77 K, which are obtained as the difference in polarization values P_1 – P_3 and P_2 – P_4 . The figures shows that these loops indicate

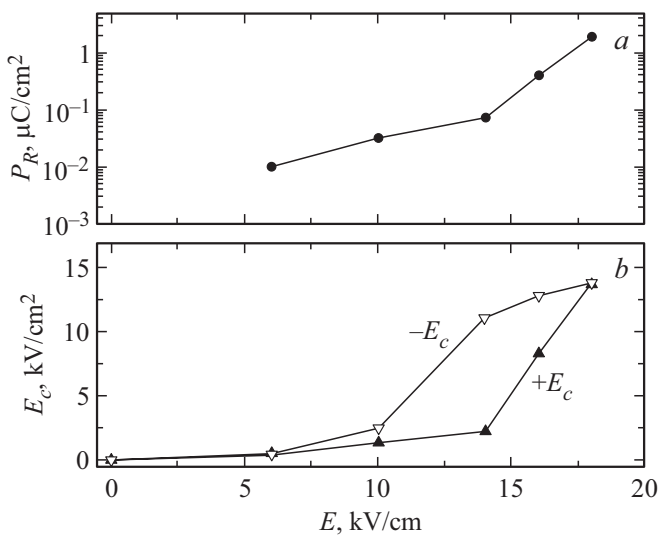


Figure 6. Dependences of residual polarization (a) and coercive field (b) in NBMN crystal on the external field from the external field.

the existence of switchable polarization and demonstrate the curve of dependence of maximum polarization on the field characteristic of ferroelectric hysteresis (shown by a dashed line in Figure 5, b). However, judging by the fact that the magnitude of the residual polarization and the coercive field increase all the time with the increase of the field amplitude up to the breakdown values ~ 20 kV/cm, it can be assumed that P–E loops are unsaturated (Figure 5, b and Figure 6).

Unsaturated hysteresis loops are also observed in most ferroelectric relaxors [1–3]. The residual polarization reaches the value of $2 \mu\text{C}/\text{cm}^2$ in the pre-breakdown external field of 18 kV/cm, and the coercive field is 14 kV/cm (Figure 6). A reversible breakdown of the crystal is observed at temperatures above 77 K due to the active accumulation of a space charge. Apparently, the impact of the space charge also affects the asymmetry of the loops in a field with an amplitude less than 18 kV/cm. According to [28] this kind of asymmetry of hysteresis loops is often attributable to the fact that the bound charge in the crystal is partially compensated by a space charge before polarization switching. The asymmetric spatial distribution of the space charge creates an internal field that affects the value of the threshold field during the polarization switching process.

4. Conclusion

This paper presents the results of the synthesis and study of a new compound — a single crystal of complex perovskite $(\text{Na}_{1/2}\text{Bi}_{1/2})(\text{Mg}_{1/3}\text{Nb}_{2/3})\text{O}_3$. The X-ray fluorescence analysis confirmed its composition, and X-ray diffraction studies determined the structure of the NBMN crystal at room temperature as cubic, space group $Pm\bar{3}m$, $a = 3.954 \pm 0.001 \text{ \AA}$. Thus, the work for the synthesis of new compounds allowed for the first time gro-

wing a single crystal of perovskite with disordering in both A- and B-sublattices. The crystal refractive index $n = 2.31 \pm 0.02$ at the wavelength of $\lambda = 0.633 \mu\text{m}$ was determined. It was shown that two anomalies with temperatures of $T_2 \approx 300 \text{ K}$ and $T_m \approx 110 \text{ K}$ are observed in the temperature dependence of the dielectric response of NBMN. The maximum in the vicinity of T_2 is frequency independent and can be associated with a structural phase transition. A wide frequency-dependent maximum in the vicinity of 110 K is characteristic of the occurrence of a relaxor ferroelectric state in the crystal with $T < T_m$. The PUND method revealed a polarization switching in the NBMN crystal at 77 K with a residual polarization $P_r = 2 \mu\text{C}/\text{cm}^2$ in 18 kV/cm field and the coercive field of $E_c = 14 \text{ kV}/\text{cm}$, which indicates the existence of a ferroelectric state. Thus, the NBMN crystal at T_m really goes into the relaxor ferroelectric state.

The dispersion of the imaginary dielectric susceptibility, $d\varepsilon''/d\omega$, changes the sign in the temperature range of 290–350 K, indicating a change of the mechanism of dielectric losses, possibly associated with a change of the nature of the conductivity of the crystal from local to bulk. This is confirmed by the analysis of temperature and frequency dependences of conductivity. An anomaly of the conductivity in the vicinity of 530 K, which is responsible for the abnormal behavior of the dielectric response, requires additional study.

The results obtained make it possible to attribute NBMN to the family of relaxor ferroelectrics and are of interest for further understanding of the mechanisms of phase transitions and transformations in partially disordered dielectric crystals. In the applied aspect, NBMN single crystals can be considered as a promising multifunctional material for integrated electronics.

Funding

This study was financed under the state assignment of the Ministry of Education and Science of the Russian Federation (topic FFUG-2024-0042).

Conflict of interest

The authors of this paper declare that they have no conflict of interest.

References

- [1] G.A. Smolensky, V.A. Bokov, V.A. Isupov, N.N. Kraynik, R.E. Pasynkov, M.S. Shur. *Segnetoelektriki i antisegetoelektriki*. Nauka, L. (1971). 476 s. (in Russian).
- [2] L.E. Cross, *Ferroelectrics* **151**, 305 (1994).
- [3] G.A. Smolensky, V.A. Isupov, A.I. Agranovskaya, N.N. Kraynik. *FTT* **2**, 2982 (1960).
- [4] A.A. Bokov, Z.G. Ye. *J. Mater. Sci.* **41**, 31 (2006).
- [5] R.A. Cowley, S. Gvasaliya, S.G. Lushnikov, B. Roessli, G.M. Rotaru. *Adv. Phys.* **60**, 229 (2011).

- [6] J.F. Scott. *Annu. Rev. Mater. Res.* **41**, 229 (2011).
- [7] H. Palneedi, M. Peddigari, G.-T. Hwang, D.-Y. Jeong, J. Ryu. *Adv. Funct. Mater.* **28**, 1803665 (2018).
- [8] X. Gao, J. Yang, J. Wu, X. Xin, Z. Li, X. Yuan, X. Shen, S. Dong. *Adv. Matter. Technol.* **5**, 1900716 (2019).
- [9] S. Nomura, K. Uchino, R.E. Newnham. **23**, 187 (1980).
- [10] T. Takenaka, K. Maruyama, K. Sakata. *Jpn. J. Appl. Phys.* **30**, 2236 (1991).
- [11] S.B. Vakhrushev, V.A. Isupov, O.E. Kvyatkovsky, N.M. Okuneva, I.P. Pronin, G.A. Smolensky, P.P. Syrnikov. *Ferroelectrics* **63**, 153 (1985).
- [12] G.O. Jones, P.A. Thomas. *Acta Cryst. B* **58**, 168 (2002).
- [13] J. Petzelt, S. Kamba, J. Fabry, D. Noujini, V. Porokhonsky, A. Pashkin, I. Franke, K. Roleder, J. Suchanicz, R. Klein, G.E. Kugel. *J. Phys.: Cond. Matter* **16**, 2719 (2004).
- [14] V. Dorcet, G. Trolliard, P. Boullay. *Chem. Mater.* **20**, 5061 (2008).
- [15] C.-S. Tu, I.G. Siny, V.H. Schmidt. *Phys. Rev.* **49**, 11550 (1994).
- [16] S. Gorfman, P.A. Thomas. *J. Appl. Cryst.* **43**, 1409 (2010).
- [17] V.G. Zalessky, A.D. Polushina, E.D. Obozova, A.V. Dmitriev, P.P. Syrnikov, S.G. Lushnikov. *Pis'ma ZhETF* **105**, 175 (2017). (in Russian).
- [18] X. Wang, H.L.W. Chan, C.L. Choy. *J. Am. Ceram. Soc.* **86**, 1809 (2003).
- [19] H. Nagata, N. Koizumi, T. Takenaka. *Key Eng. Mater.* **169–170**, 37 (1999).
- [20] D. Lin, D. Xizo, J. Zhu, P. Yu, H. Yan, L. Li, W. Zhang. *Cryst. Res. Technol.* **39**, 30 (2004).
- [21] S.E. Park, S.J. Chung, I.T. Kim, K.S. Hong. *J. Am. Ceram. Soc.* **77**, 2641 (1994).
- [22] X. Wang, S. Or, X. Tang, H. Chan, P. Choy, P. Liu. *Solid State Commun.* **134**, 659 (2005).
- [23] H. Yan, D. Xiao, P. Yu, J. Zhu, D. Lin, G. Li. *Mater. Des.* **26**, 474 (2005).
- [24] Y. Yamada, T. Akutsu, H. Asada, K. Nozawa, S. Hachiga, T. Kurosaki, O. Ikagawa, H. Fujiki, K. Hozumi, T. Kawamura, T. Amakawa, K. Hirota, T. Ikeda. *Jpn. J. Appl. Phys.* **34**, 5462 (1995).
- [25] S.R. McLaughlin. PhD thesis. Queen's University Kingston, Ontario, Canada (2008). 139 p.
- [26] D. O'Neill, R.M. Bowman, J.M. Gregg. *Appl. Phys. Lett.* **77**, 1520 (2000).
- [27] K.M. Rabe, C.H. Ahn, J.-M. Triscone. *Physics of Ferroelectrics. A Modern Perspective*. Springer-Verlag, Berlin Heidelberg (2007). 388 p.
- [28] K. Okazaki. *Ceramic Engineering for Dielectric*. Gakkensha, Tokyo (1969). 532 p.

Translated by A.Akhtyamov